Published by
NIGERIAN SOCIETY OF PHYSICAL SCIENCES
Available online @ https://journal.nsps.org.ng/index.php/jnsps

J. Nig. Soc. Phys. Sci. 8 (2026) 3087

Journal of the Nigerian Society of Physical Sciences

A comprehensive investigation of dual-damped Euler-Bernoulli beam under moving mass on Pasternak foundation via spectral and central difference methods

Adebola Samuel Adeoye[a], Ezekiel Olaoluwa Omole[b,*], Sule Adekunle Jimoh[a], Victoria Iyadunni Ayodele[c], Taiwo Aanu Ogunlusi[d]

[a]*Department of Mathematical Sciences, Achievers University, Owo, Ondo State, Nigeria*
[b]*Department of Mathematics, Federal University of Technology and Environmental Sciences, Iyin-Ekiti, Ekiti State, Nigeria*
[c]*Department of Computer Science and Mathematics, Nigeria Police Academy, Wudil,Kano State, Nigeria*
[d]*Department of Mathematics, Federal University of Oye-Ekiti, Ekiti State, Nigeria*

Abstract

This study investigates the dynamic behavior of a dual-damped Euler-Bernoulli beam carrying a moving mass and supported on a Pasternak foundation, with the aim of improving prediction and control of vibration in structural systems. The beam model incorporates both internal (material) and external (viscous) damping and is discretized spatially using the Chebyshev collocation method (high-order spectral accuracy). Time integration is performed with an explicit central-difference scheme. Convergence and stability of the high-order spatial discretization with explicit time stepping are assessed, and extensive parametric studies are carried out over inertia, foundation shear stiffness, and damping coefficients. Numerical results validated across simulation cases show clear repeatable trends: increases in mass per unit length, foundation shear stiffness, and viscoelastic (internal and external) damping all substantially reduce peak deflection amplitudes and mid-span displacement. The moving-mass model predicts lower critical speeds and larger dynamic amplification better than equivalent moving-force approximations. The combined dual-damped, high-order numerical scheme provides an accurate efficient tool for analyzing beam dynamics under moving loads. Results highlight practical design levers (inertia, shear stiffness, damping) that engineers can tune to mitigate vibration in civil, structural, and biomechanical applications, and identify parameter ranges most susceptible to resonance.

DOI:10.46481/jnsps.2026.3087

Keywords: Euler-Bernoulli beam, Chebyshev collocation, Central difference, Damping coefficients, Pasternak foundation

Article History :
Received: 11 August 2025
Received in revised form: 26 January 2026
Accepted for publication: 08 February 2026
Available online: 14 May 2026

Communicated by: P. Thakur

1. Introduction

In the modern era of high-speed transportation, intelligent infrastructure, and responsive structural systems, the need for precise and predictive dynamic modeling of engineering structures under complex loading conditions has never been more critical. Beams, ubiquitous in bridges, railways, aerospace structures, and biomedical frameworks, are frequently subjected to moving loads, demanding accurate prediction of their dynamic behavior to ensure safety, comfort, and longevity. Yet, traditional approaches often fall short when confronted with the multi-faceted realities of foundation flexibility, material damping, and time-dependent moving forces. It is within this intricate domain that the present study carves a novel and vital

*Corresponding author: Tel.: +234-806-508-6963
Email address: omolez247@gmail.com (Ezekiel Olaoluwa Omole)

contribution.

The classical Euler–Bernoulli beam theory, despite its foundational role in structural mechanics, assumes an idealized, often undamped behavior resting on simplistic support conditions. However, real-world systems are rarely so ideal. Damping mechanisms, both external (viscous) and internal (structural or material), play significant roles in governing how energy is absorbed, transferred, or dissipated under dynamic loads. Ignoring these dual damping effects can lead to underestimation of critical deflections or misjudgment of the fatigue life of a structure. The foundation upon which a structure rests dramatically influences its vibrational response. While the Winkler model has traditionally been employed for its simplicity, idealizing the foundation as a set of independent springs, it fails to capture shear interactions between adjacent support points. The Pasternak foundation, which augments the Winkler model by introducing a shear layer characterized by a shear modulus, provides a more physically realistic representation of ground–structure interaction. This dual-parameter foundation model captures both vertical stiffness and shear deformation, enabling a more nuanced understanding of soil–structure and interface dynamics.

To elevate the analysis to modern engineering standards, this research integrates these complex physical features into a dual-damped Euler–Bernoulli beam model resting on a Pasternak foundation and subjected to a distributed moving mass. Solving such a system analytically is formidable, if not impossible. Hence, Chebyshev collocation is adopted as a high-precision spectral method for spatial discretization. This approach exploits the superior convergence properties of Chebyshev polynomials and their associated differentiation matrices, ensuring that even small-scale variations in displacement or stress fields are captured with minimal computational cost. In the time domain, the Central Difference Method (CDM), a widely adopted explicit numerical scheme, is employed for its efficiency and simplicity in solving second-order differential equations. The synergy between Chebyshev spectral discretization and CDM enables accurate and computationally tractable simulation of the transient response of the system.

Unlike low-order finite element (FEM) or finite difference methods, Chebyshev collocation is a global spectral technique in which the beam response is approximated using high-order Chebyshev polynomials over the entire spatial domain. In elastic vibration problems, the discretization error decays exponentially with the number of collocation points. Boundary conditions are enforced strongly and exactly at the collocation points without reformulation of shape functions or remeshing. Moreover, Chebyshev collocation avoids spurious boundary layers and numerical leakage near supports. The CDM, being explicit, requires no Newton iterations and avoids numerical damping unless it is physically present, thereby preserving the true dynamic interaction between the structure and the moving mass. In contrast, implicit schemes such as Newmark-β and generalized-α methods require matrix refactorization at every time step, increasing computational cost and algorithmic complexity. CDM handles time-varying coefficients naturally and avoids iterative solvers and convergence issues, remaining stable and efficient even under strong inertia coupling. This unified framework allows stability, convergence, and resonance phenomena to be analyzed consistently within the same mathematical structure.

Several studies have been conducted on structural members resting on elastic foundations. Early formulations sought to overcome the limitations of simple Winkler-type assumptions [1]. The introduction of two-parameter foundation models provided a more realistic description of soil–structure interaction by incorporating shear deformation effects [2]. Subsequent refinements introduced improved representations of elastic continuity and viscoelastic behavior in supporting media [3]. Further developments extended these models to include enhanced mechanical realism and refined constitutive relations [4]. More recently, generalized and nonlocal foundation models incorporating long-range interactions and fractional-order formulations have been proposed to capture complex soil behavior with higher fidelity [5]. Comprehensive investigations on viscoelastic dampers and foundation-supported structural dynamics further emphasize the importance of realistic foundation modeling in vibration problems [6, 7].

The dynamic behavior of structural elements resting on elastic foundations under moving loads has been widely studied. In particular, the response of orthotropic plates and beams subjected to moving distributed masses on bi-parametric foundations has confirmed that the combined effects of inertia coupling, foundation shear stiffness, and anisotropy can significantly alter vibration amplitudes and resonance characteristics [8]. Reviews on elastic and viscoelastic foundation models have demonstrated that variable foundation parameters are essential for accurate prediction of dynamic responses [9]. In addition, the influence of functionally graded materials and two-parameter elastic foundations under moving mass excitation has been shown to be substantial [10].

The incorporation of damping into beam models has attracted considerable attention. Fundamental vibration theory establishes the governing role of damping in controlling resonance amplitudes and transient decay rates [11]. Variational principles provide a consistent mathematical framework for embedding damping and foundation effects into structural models [12]. Hysteretic internal damping in laminated and composite beams has been examined in detail [13], while classical texts on structural dynamics emphasize the correct interpretation of physical damping versus algorithmic numerical dissipation [14]. The mechanical behavior of viscoelastic materials and frequency-dependent damping has been systematically described [15]. Fractional-order constitutive models further extend damping representation by accounting for memory effects and complex energy dissipation mechanisms [16]. Classical time integration algorithms for structural dynamics were introduced by Newmark [17], followed by improved formulations incorporating numerical dissipation control [18] and the generalized-α method [19]. These developments form the backbone of modern computational structural dynamics and are standard in finite element formulations [20].

The problem of beams subjected to moving loads and moving masses remains central to vibration engineering. Frýba's

monograph continues to serve as a seminal reference on structural vibration under moving loads [21]. Vehicle–bridge interaction dynamics and the distinction between moving force and moving mass models were clarified in pioneering works [22]. Nonlinear coupled dynamics of beam–mass systems under moving loads have been investigated to capture inertia coupling and large-amplitude responses [23]. Comprehensive treatments of moving load analysis and identification techniques are also available in monograph form [24]. The vibration of orthotropic plates resting on Pasternak foundations under moving distributed masses has been explored, highlighting the strong role of foundation shear stiffness and mass inertia [25]. Parametric excitation induced by intermittent passage of moving masses has been shown to generate instability and resonance phenomena [26]. Extensions to variable Pasternak foundations under moving loads have further confirmed the sensitivity of structural response to spatial heterogeneity of soil properties [27]. Variable-velocity and accelerating moving-mass models, which mathematically represent stop-and-go excitation, have also been investigated in beam dynamics [28]. Optimal vibration control strategies for moving-mass beam systems under uncertainty have been developed [29]. More recently, machine-learning approaches have been applied to predict vibration performance and structural comfort under dynamic loading conditions [30].

From the numerical perspective, spectral methods provide exceptional accuracy for smooth structural vibration problems. Trefethen popularized Chebyshev spectral techniques and demonstrated their exponential convergence properties [31]. A comprehensive theoretical framework for spectral methods was provided by Canuto *et al.* [32], while algorithmic and implementation aspects were developed in subsequent monographs [33]. Differentiation matrix construction and pseudospectral techniques were rigorously analyzed in computational mathematics literature [34, 35]. Quadrature efficiency and spectral accuracy properties were investigated in detail [36]. Numerical linear algebra foundations essential for stability and conditioning of spectral discretizations were established in classical references [37, 38]. Practical guides to pseudospectral implementations and Fourier–Chebyshev methods are also well documented [39, 40].

The CDM remains one of the most powerful explicit time-integration schemes in structural dynamics. Its stability, simplicity, and energy-conserving properties were significantly enhanced by the generalized-α framework [41]. Finite element formulations and transient integration strategies were rigorously established in classical texts [42]. Variable-step central difference methods were introduced to improve efficiency and stability [43, 44]. Explicit schemes with optimal numerical dissipation were later proposed to further enhance numerical robustness [45].

Recent developments include improved Pasternak foundation formulations accounting for generalized shear forces [46], simplified dynamic analysis of beam–column elements on non-homogeneous Pasternak foundations [47], and layered composite beam responses under shock excitation including structural damping and stiffness effects [48]. Studies on composite materials with periodic fiber waviness have provided important insight into stiffness degradation and failure mechanisms [49]. High-order multistep collocation techniques have been proposed for solving partial differential equations arising in fluid and solid mechanics [50]. Natural vibration analysis of axially graded tapered beams on bi-parametric elastic foundations has also been carried out [51], while the response of non-prismatic Euler–Bernoulli beams resting on variable elastic foundations has been examined in detail [52]. The classical monograph on vibration of solids and structures under moving loads remains indispensable for understanding the theoretical foundations of moving load problems [53].

Few works in the literature have combined spectral spatial discretization with explicit time integration for moving-mass beam problems due to perceived stability concerns. This work demonstrates that the proposed solution technique is both accurate and robust when properly implemented. Most FEM and modal approaches smear the moving mass over elements or truncate high-frequency modal contributions, whereas Chebyshev collocation captures localized effects through global basis functions and avoids mesh-locking and load smearing. The convergence behavior of the methods adopted in this work is predictable, verifiable, and theoretically supported, which strengthens their numerical credibility, since the methods enable spectral convergence in space and second-order convergence in time. Therefore, this study addresses these gaps by offering an effective solution to the beam problem through the combination of the two aforementioned techniques. The accuracy and stability of this solution approach can help engineers to predict, control, and ultimately innovate across a full spectrum of dynamic structural applications by uniting high-order spectral methods, realistic damping physics, and foundation coupling under a moving mass.

2. Euler-Bernoulli model

The Euler-Bernoulli beam model [EBBM] is sometimes called the “classical beam theory”. provides a remarkably simple but yet powerful way to predict the behaviour of slender beams under loads.

Under a distributed transverse load, $q(x)$ (force per length), the static deflection $w(x)$ satisfies

$$EI\frac{d^4w}{dx^4} = q(x), \tag{1}$$

where E is the Young’s modulus, I is the second moment of area (about the neutral axis) and $w(x)$ is the transverse deflection. For dynamic motion (no damping, no foundation) but with inertia, we have

$$EI\frac{d^4w}{dx^4} + \rho A\frac{\partial^2}{\partial t^2} = q(x,t), \tag{2}$$

where ρA is the mass per unit length and $q(x)$ is the time-varying transverse loading.

2.1. Beam governing equation

The governing equation for the transverse motion, $w(x,t)$, of the dynamic behavior of Bernoulli-Euler beam with dual-parameter damping under moving distributed masses on a Pasternak foundation with trigonometric loading is formulated as:

$$EI\frac{\partial^4}{\partial x^4}u(x,t) + C_{\text{ex}}\frac{\partial}{\partial t}u(x,t) + \eta_{\text{int}}\frac{\partial^3}{\partial x^2\partial t}u(x,t) + m_b \frac{\partial^2}{\partial t^2}u(x,t) + K_o u(x,t) + G_o\frac{\partial^2}{\partial x^2}u(x,t) = p(x,t), \quad (3)$$

where $u(x,t)$ = transverse displacement of the beam, E = Young's modulus of elasticity, EI = flexural rigidity of the beam, m_b = mass per unit length of the beam, C_{ex} = external damping coefficient (velocity-dependent damping), η_{int} = higher-order damping coefficient (accounts for frequency-dependent damping), K_o = Winkler foundation stiffness, G_o = Pasternak foundation shear parameter and $p(x,t)$ = load distribution function due to the moving distributed masses.

If a moving distributed mass m_d with velocity v is present over a length, the loading function can be expressed as:

$$p(x,t) = m_d\delta(x-vt)\left(\frac{\partial^2}{\partial x^2}u(x,t) + 2v\frac{\partial^2}{\partial x\partial t}u(x,t) + v^2\frac{\partial^4}{\partial x^4}u(x,t)\right) + q(x,t), \quad (4)$$

where $\delta(x-vt)$ = Dirac delta function representing the moving mass which is defined as:

$$\delta(x-vt) = \frac{1}{L_x}\left[1 + 2\sum_{n=1}^{\infty}\cos\left(\frac{nvt}{L_x}\right)\cos\left(\frac{nvx}{L_x}\right)\right], \quad (5)$$

$q(x,t)$ = external force acting on the beam, $q(x,t)$ = external force acting on the beam and m_d is the mass of the external body traversing.

The mass per unit length can be expressed as:

$$m_b = \rho A = \frac{m}{V}A, \quad (6)$$

where m is the mass of the beam, V is its volume and A its area.

In general, $EI\frac{\partial^4}{\partial x^4}u(x,t)$ represents the bending stiffness, $C_{\text{ex}}\frac{\partial}{\partial t}u(x,t)$ represents structural damping, $\eta_{\text{int}}\frac{\partial^3}{\partial x^2\partial t}u(x,t)$ accounts for frequency-dependent damping, $m_b\frac{\partial^2}{\partial t^2}w(x,t)$ represents the inertial effect of the beam, $K_o u(x,t)$ represents the Winkler foundation restoring force, $-G_o\frac{\partial^2}{\partial x^2}u(x,t)$ represents the shear interaction in the Pasternak foundation and $p(x,t)$ represents the effect of moving distributed masses and external force.

In the governing equation of the problem, internal damping acts on the rate of curvature (ie. bending strain rate), foundation shear stiffness couples to curvature and acts like a gradient-dependent stiffness. This smooths the spatial response, resits curvature and spreads a concentrated load over a larger region compared to pure Winkler term and moving mass supplies a localized, time-dependent inertial load that depends on the structure's local acceleration. It therefore injects energy into the structure at moving location.

2.2. Boundary and initial conditions

The Chebyshev collocation method inherently applies the differential operator at interior nodes. The clamped end boundary conditions imply both displacement and slope varnish:

$$u = 0 = \frac{\partial u}{\partial x}. \quad (7)$$

The initial conditions, without any loss of generality, is expressed as

$$u = 0 = \frac{\partial u}{\partial t}. \quad (8)$$

3. Method of solution

The governing equation of this work is solved firstly with Chebyshev collocation for discretization and thereafter, with the central difference method for the time dependent solution for the deflection.

3.1. Chebyshev collocation discretization

Firstly, Chebyshev collocation method is used to discretize the governing equation. Doing so helps in providing high accuracy with relatively few collocation points. The following steps are required in discretizing the governing equation by the Chebyshev collocation method:

i **Chebyshev nodes and differentiation matrices**
The domain is mapped spatially in the interval, $x \in [-1,\ 1]$ or in any other interval through an appropriate transformation. For a given number $N+1$ of collocation points, the Chebyshev-Gauss-Lobatto nodes are defined as:

$$x_j = \cos\left(\frac{j\pi}{N}\right),\ j = 0,\ 1,\ \ldots,\ N. \quad (9)$$

We construct the Chebyshev differentiation matrix D which approximates the first derivative at the collocation points. Higher derivatives are then obtained by matrix powers:

$$D^{(k)} \approx D^k, \quad k = 2,3,4. \quad \frac{\partial}{\partial x}u \approx D\boldsymbol{U}, \quad \frac{\partial^2}{\partial x^2}u \approx D^2\boldsymbol{U}, \quad \frac{\partial^4}{\partial x^4}u \approx D^4\boldsymbol{U}, \quad (10)$$

where D^k are the Chebyshev differentiation matrices (with $k = 2,\ 3,\ 4$ as needed).

ii **Discretization of the governing equations**
At the collocation points x_j, the differential operators are replaced by the corresponding matrices. Denoted by $\boldsymbol{U}(t)$ the vector of nodal values. The spatial derivatives become:

$$EI\frac{\partial^4}{\partial x^4}u\left(x_j,t\right) \longrightarrow EI\left(D^4\boldsymbol{U}\right)(j),$$

$$-G_o\frac{\partial^2}{\partial x^2}u\left(x_j,t\right) \longrightarrow -G_o\left(D^2\boldsymbol{U}\right)(j)$$

$$K_o u\left(x_j,t\right) \longrightarrow K_o u_j(t), \quad C_{\text{ex}}\frac{\partial}{\partial t}u(x,t) \longrightarrow C_{\text{ex}}\dot{u}_j(t)$$

$$\eta_{\text{int}} \frac{\partial^3}{\partial x^2 \partial \text{t}} u\left(x_j, t\right) \longrightarrow \eta_{\text{int}} \left(D^2 \dot{\boldsymbol{U}}\right)(j),$$

$$m_b \frac{\partial^2}{\partial t^2} u\left(x_j, t\right) \longrightarrow m_b \ddot{u}_j(t). \tag{11}$$

All these are evaluated at the nodes.
Thus, the discretized equation at each node becomes:

$$[EI\left(D^4 \boldsymbol{U}\right)(j) + C_{\text{ex}} \dot{u}_j(t) + \eta_{\text{int}}\left(D^2 \dot{\boldsymbol{U}}\right)(j) + m_b \ddot{u}_j(t) + K_o w_j(t)] - G_o\left(D^2 \boldsymbol{U}\right)(j) = q\left(x_j, t\right), \tag{12}$$

which is further rewritten as:

$$[EID^4 \boldsymbol{U}(t) - G_o D^2 \boldsymbol{U}(t) + K_o \boldsymbol{U}(t) + C_{\text{ex}} \dot{\boldsymbol{U}}(t)] + \eta_{\text{int}} D^2 \dot{\boldsymbol{U}}(t) + m_b \ddot{\boldsymbol{U}}(t) = \boldsymbol{q}(t). \tag{13}$$

iii **Imposing the boundary conditions**
The Chebyshev collocation method inherently applies the differential operator at interior nodes. The clamped end boundary conditions in equation 7 are incorporated.
At the endpoints, boundary conditions are enforced by modifying the system and replacing rows in the differentiation matrices corresponding to the boundary nodes with the conditions.
For instance, if the beam is clamped at $x \pm 1$, then set:

$$u(x_o,\ t) = u(x_N,\ t) = 0,$$
$$(D\boldsymbol{U})(x_o,\ t) = (D\boldsymbol{U})(x_N,\ t) = 0. \tag{14}$$

The resulting system is a set of second order ordinary differential equations (ODEs) in time as expressed

$$m_b J\, \ddot{\boldsymbol{U}}(t) + \left(C_{\text{ex}} J + \eta_{\text{int}} D^2\right) \dot{\boldsymbol{U}}(t) + \left(EID^4 - G_o D^2 + K_o J\right) \boldsymbol{U}(t) = \boldsymbol{q}(t). \tag{15}$$

The above system of equations is solved using the central difference method which is a powerful time-stepping method. The moving load $\boldsymbol{q}(t)$ is updated at each time step by evaluating the load distribution at the current location of the moving mass.

3.2. The central difference method

The semi-discretized system is then solved using the central difference method. After the application of Chebyshev collocation method, the beam's dynamics become a second-order system in time, t, that can be written in matrix-vector form as

$$M\, \ddot{\boldsymbol{U}}(t) + C\, \dot{\boldsymbol{U}}(t) + K\, \boldsymbol{U}(t) = \boldsymbol{q}(t), \tag{16}$$

where $M = m_b$, which is the mass matrix, $C = \left(C_{\text{ex}} J + \eta_{\text{int}} D^2\right)$, which is the damping matrix,

$K = \left(EID^4 - G_o D^2 + K_o J\right)$, which is the stiffness matrix $\boldsymbol{U}(t)$ is the vector of displacements at the collocation nodes. The forcing term $\boldsymbol{q}(t)$ includes the effects of the moving distributed masses (and any additional external load) and J denotes a unit matrix.
The central difference method is one of the most straightforward and yet powerful time integration scheme for second-order dynamical system of the form above. The method is explained step by step as below

a **Finite-difference approximations**
We discretize time into uniform steps of size $\triangle t$, so $t_n = n\triangle t$. The central difference approximations are

- command **Acceleration at step *n* :**

$$\ddot{\boldsymbol{U}}^n = \frac{d^2 \boldsymbol{U}}{dt^2} \approx \frac{\boldsymbol{U}^{n+1} - 2\boldsymbol{U}^n + V^{n-1}}{\Delta t^2}, \tag{17}$$

- command **Velocity at step*n*:**

$$\dot{\boldsymbol{U}}^n \approx \frac{\boldsymbol{U}^{n+1} - \boldsymbol{U}^{n-1}}{2\Delta t}. \tag{18}$$

b **Discrete equation of motion** Substituting the acceleration and velocity approximations into the discretize equation, we have

$$M\left[\frac{\boldsymbol{U}^{n+1} - 2\boldsymbol{U}^n + \boldsymbol{U}^{n-1}}{\Delta t^2}\right] + C\left[\frac{\boldsymbol{U}^{n+1} - \boldsymbol{U}^{n-1}}{2\Delta t}\right] + K\, \boldsymbol{U}^n = \boldsymbol{q}^n. \tag{19}$$

Rearranging and rewriting, we have

$$W^{n+1}\left[M + \frac{\Delta t}{2} C\right] = \Delta t^2 q^n + \left[2M - \Delta t^2 K\right] \boldsymbol{U}^n - \left[M - \frac{\Delta t}{2} C\right] \boldsymbol{U}^{n-1}, \tag{20}$$

which is further rewritten as

$$\boldsymbol{U}^{n+1} = {M_{\text{eff}}}^{-1} R^n, \tag{21}$$

where $M_{\text{eff}} = M + \frac{\Delta t}{2} C$which is mostly diagonal and $R^n = \left[2M - \Delta t^2 K\right] \boldsymbol{U}^n - \left[M - \frac{\Delta t}{2} C\right] \boldsymbol{U}^{n-1}$

c **Initialization** To start the recurrence, we need:

- command $\boldsymbol{U}^0$ from initial displacement
- command $\dot{\boldsymbol{U}}^0$ from initial velocity

We compute W^1 via a Taylor expansion at $t = 0$:

$$\boldsymbol{U}^1 = \boldsymbol{U}^0 + \Delta t \dot{\boldsymbol{U}}^0 + \frac{\Delta t^2}{2} \ddot{\boldsymbol{U}}^0, \ddot{W}^0 = M^{-1}\left[q^n - C\dot{W}^0 - KW^0\right]. \tag{22}$$

4. Numerical error analysis and convergence study

4.1. Numerical error analyses

4.1.1. Spectral (spatial truncation) error

This error arises from approximating the continuous field $w(x)$ by a truncated Chebyshev expansion of order N. Let $w_N(x)$ denote the spectral approximation of $w(x)$. The spectral truncation error is defined as:

$$\|w - w_N\| \leq Ce^{-\alpha N}, \qquad (C, \alpha > 0), \tag{23}$$

which demonstrates exponential convergence with respect to the polynomial order N, provided the exact solution is sufficiently smooth. This exponential decay of error is one of the major advantages of spectral methods over low–order discretization techniques such as finite difference and finite element methods.

4.1.2. Differentiation matrix conditioning and round-off amplification

This error arises due to the loss of numerical accuracy when spectral differentiation matrices become ill-conditioned, particularly for higher–order derivatives. As the number of collocation points N increases, the condition number of the differentiation matrices grows rapidly, leading to amplification of round-off errors.

The conditioning of the m-th order differentiation matrix $D^{(m)}$ is typically expressed as:

$$\kappa\left(D^{(m)}\right) \sim CN^{2m}, \tag{24}$$

where:

- $\kappa(D^{(m)})$ is the condition number of the m-th order differentiation matrix,
- N is the number of spectral collocation points,
- m is the order of differentiation,
- C is a problem–dependent constant.

This relationship shows that the condition number increases rapidly with both N and the derivative order m, making high–order derivatives particularly sensitive to numerical round-off errors and loss of precision.

4.1.3. Temporal truncation error

The temporal truncation error arises from approximating time derivatives using finite difference schemes, such as the CDM. It represents the error introduced by discretizing the time variable.

The local truncation error is given by

$$E_{\text{local}} = C_t\,\Delta t^3, \tag{25}$$

while the global temporal discretization error is of second order, expressed as

$$E_{\text{time}} = O(\Delta t^2), \tag{26}$$

where Δt is the time step size and C_t is a problem–dependent constant that depends on higher–order time derivatives of the exact solution.

The constant C_t is precisely defined as

$$C_t = \frac{1}{12}\max_{t\in[t_n,\,t_{n+1}]}\left|\frac{d^3u(t)}{dt^3}\right|. \tag{27}$$

This expression shows that the magnitude of the temporal truncation error is governed by the third–order time derivative of the exact solution and the cube of the time step size.

4.2. Convergence study

4.2.1. Spatial convergence

For sufficiently smooth solutions, the Chebyshev spectral method exhibits exponential (spectral) convergence, as illustrated in Fig. 1. The error is computed relative to a highly resolved numerical solution used as the reference solution. When

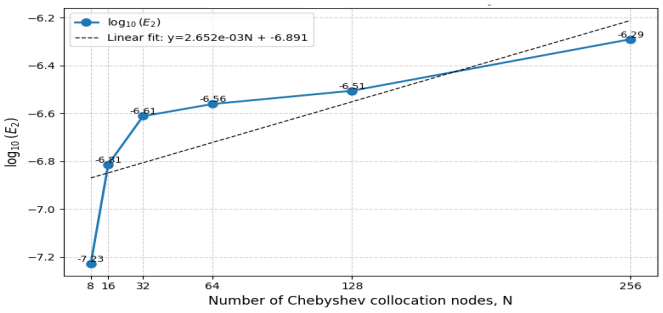

Figure 1: Spatial Convergence Curve

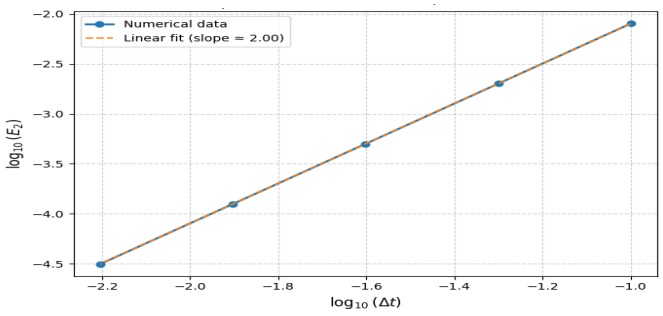

Figure 2: Temporal convergence study

N becomes very large, the conditioning of the stiffness matrix deteriorates and the condition number cond(K) may reach values between 10^{10} and 10^{15}. In this regime, round-off errors may dominate the numerical solution.

For non-smooth solutions or problems involving localized loads, the convergence behaviour degrades from exponential to algebraic.

The figure demonstrates spectral convergence of the Chebyshev collocation method for Euler-Bernoulli beam. A dashed linear fit shows that over the fitted range of N, the error follows an exponential (spectral) decay of the form $E_2(N) \approx Ce^{-\alpha N}$, $\log E_2(N) = mN + b$, where $m = -\frac{\alpha}{\ln 10}N$ is the fitted slope which represents the decay and $b = \log C$ is the intercept. From the slope, $\alpha = -m \ln 10$

4.2.2. Temporal convergence

For the temporal convergence study, the error E_2 is evaluated for decreasing time steps Δt, and $\log(E_2)$ is plotted against $\log(\Delta t)$. As shown in Fig. 2, the results form an almost straight line on the log–log scale, indicating second–order temporal convergence of the central difference method (CDM). The slope of the fitted line is approximately $1.999 \approx 2$, confirming that the numerical error decreases quadratically with the time step size Δt, as expected for a second–order explicit time integration scheme. This also indicates that the chosen time step satisfies the stability condition, since larger values of Δt lead to numerical instability.

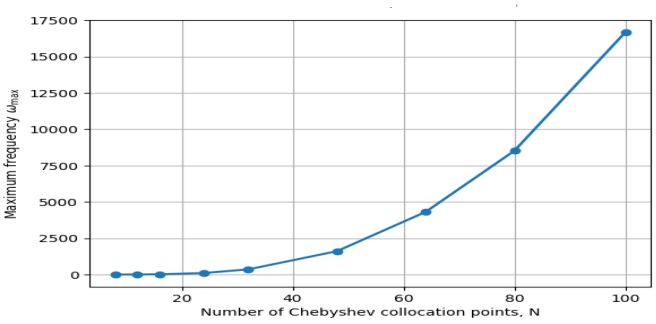

Figure 3: Variation of the maximum eigenfrequency and the corresponding stability limit with spatial resolution

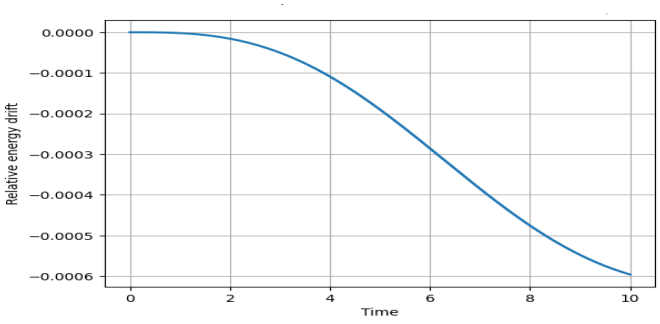

Figure 4: Relative energy drift versus time showing the energy behaviour of the numerical scheme

4.2.3. Stability metric (ω_{max} and Δt_{max})

The largest natural frequency (spectral radius) $\omega_{\max}$ of the semi-discrete system is obtained after the Chebyshev collocation discretization. It corresponds to the highest spatial mode introduced by the spectral differentiation matrices. Because Chebyshev collocation clusters points near the boundaries, the value of $\omega_{\max}$ increases rapidly as the number of collocation points N increases.

As illustrated in Fig. 3, the maximum eigenfrequency $\omega_{\max}$ grows with increasing spatial resolution, which leads to a corresponding reduction in the maximum stable time step

$$\Delta t_{\max} = \frac{2}{\omega_{\max}}.$$

This behaviour indicates that as higher spatial modes are captured, the explicit central difference scheme must use a smaller time step to maintain numerical stability.

The central difference method (CDM) is conditionally stable. For an undamped system ($C = 0$), the stability condition is

$$\Delta t \leq \frac{2}{\omega_{\max}}. \tag{28}$$

When damping is present ($C \neq 0$), the stability limit becomes slightly more restrictive. In practice, the time step Δt is therefore selected based on the highest frequency content of the semi-discrete system in order to avoid numerical instability or solution blow-up. The quantity $\omega_{\max}$ denotes the largest natural circular frequency of the system is defined as

$$\omega_{\max} = \max_i \omega_i, \tag{29}$$

where the natural frequencies ω_i are obtained from the generalized eigenvalue problem $K\phi_i = \omega_i^2 M\phi_i$, or equivalently from the characteristic equation

$$\det(K - \omega^2 M) = 0. \tag{30}$$

4.2.4. Energy conservation

The evolution of the total energy provides an important diagnostic for assessing the physical accuracy and numerical stability of the Chebyshev collocation–central difference solution framework for the Euler–Bernoulli beam under a moving mass on a Pasternak foundation. For the undamped case ($C_{ex} = \eta_{int} = 0$) and sufficiently small time step Δt, the relative energy drift $\xi(t)$ remains very small. The quantity $\frac{\Delta\xi(t)}{\xi(0)}$ is plotted against time to monitor energy conservation. As Δt decreases, the energy drift reduces, and energy is conserved to within approximately 0.2% for $\Delta t = 0.1\,\Delta t_{\max}$. When damping is included, the system becomes dissipative and the total energy decreases with time. As $\Delta t \to \Delta t_{\max}$, the energy drift increases slightly, but the decay follows a smooth exponential-type envelope.

As shown in Fig. 4, the small magnitude of the energy drift indicates that the numerical scheme is nearly energy-conserving for the undamped case, while the smooth monotonic decay confirms the expected dissipation when damping effects are present. This behaviour demonstrates the stable coupling between Chebyshev spatial discretization and central difference time integration.

Overall, the numerical error and convergence results confirm that the hybrid Chebyshev–central difference scheme provides an accurate and stable approach for transient beam dynamics when the pair $(N, \Delta t)$ satisfies the stability and convergence requirements.

5. Discussion of simulation

The numerical results obtained are used to generate meaningful graphs with some varying parameters. The deflection profile is plotted over time and then the curves show the effects of the varying parameters $EI, I, C_{\text{ext}}, \eta_{\text{int}}, m_b, h, L, , v, m, K_o$ and G_o on the deflection of the beam.

5.1. Qualitative discussion of simulated figures

(a) **Effect of Mass per Unit Length (m_b [kg m^{-1}]):** As the mass per unit length m_b increases, the peak oscillation amplitude at the beam midpoint decreases significantly, as shown in Fig. 5. A larger mass increases the system's inertia, making the beam more resistant to acceleration under the same moving load. Consequently, the beam responds more sluggishly and exhibits smaller vibration amplitudes.

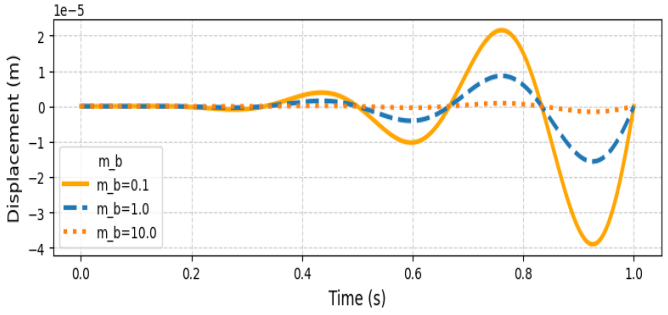

Figure 5: Effect of m_b (kg m^{-1}) on the displacement of the beam

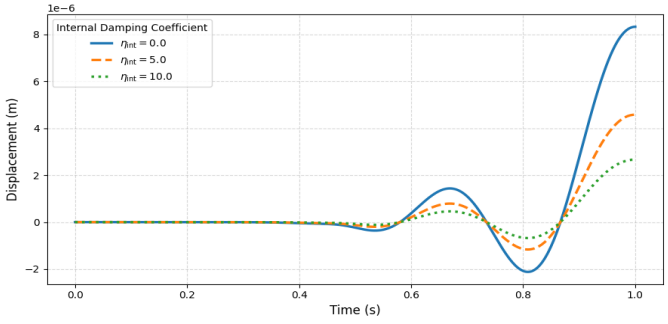

Figure 6: Effect of η_{int} (N s m^{-2}) on the displacement of the beam

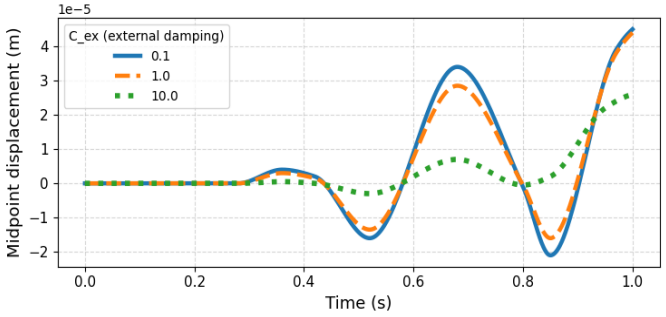

Figure 7: Effect of C_{ex} (N s m^{-2}) on the displacement of the beam

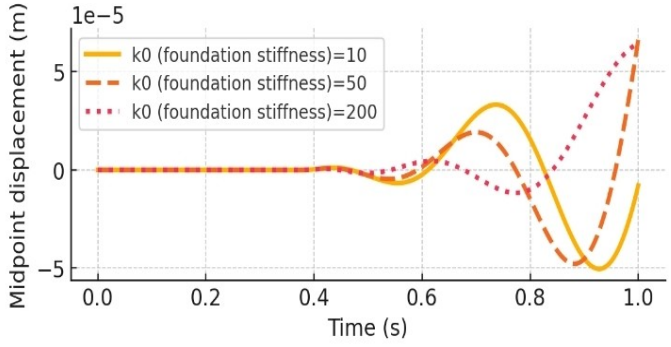

Figure 8: Effect of K_o (N m^{-3}) on the displacement of the beam

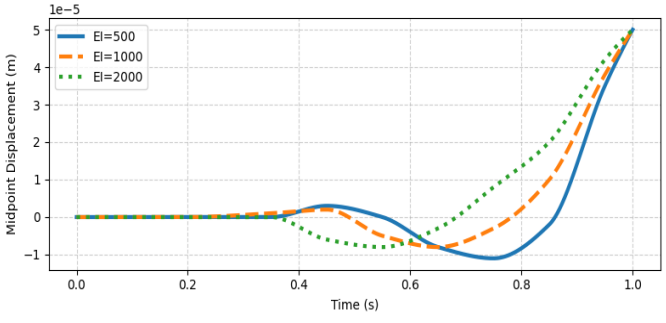

Figure 9: Effect of EI (N m^2) on the displacement of the beam

(b) **Effect of internal damping (η_{int} [N s m^{-2}]):** Without internal damping ($\eta_{int} = 0$), the beam oscillates freely and exhibits the largest vibration amplitudes. As shown in Fig. 6, increasing η_{int} reduces the oscillation peaks. For moderate damping, the amplitudes decrease noticeably, while for large damping the response becomes nearly flat. Internal (material) damping dissipates vibration energy through the viscoelastic behaviour of the beam, causing faster decay of oscillations and a significant reduction in the maximum deflection.

(c) **Effect of external damping (C_{ex} [N s m^{-2}]):** External damping accounts for energy loss from the beam to the surrounding medium. Figure 7 shows that for small values of C_{ex}, the beam responds with larger post-load oscillations. Increasing C_{ex} enhances energy dissipation, thereby reducing the peak deflection and causing the vibrations to decay more rapidly.

(d) **Effect of foundation (Winkler) stiffness (K_o [N m^{-3}]):** The Winkler stiffness K_o represents the vertical support provided by the elastic foundation. As shown in Fig. 8, when K_o is small the foundation offers little resistance, allowing the beam to deflect significantly under the moving mass. Increasing K_o strengthens the vertical support, which reduces the mid-span deflection and slightly modifies the response as the load passes the midpoint.

(e) **Effect of flexural rigidity (EI [N m^2]):** Flexural rigidity EI measures the beam's resistance to bending. As shown in Fig. 9, a small value of EI makes the beam highly flexible, resulting in larger deflections under the moving load. As EI increases, the beam becomes stiffer and resists bending more effectively. Consequently, the peak deflection decreases significantly and occurs closer to the instant when the load passes directly over the midpoint.

(f) **Effect of shear layer stiffness (G_o [N m^2]):** The shear layer stiffness G_o represents the shear interaction within the Pasternak foundation. As shown in Fig. 10, when G_o is zero the beam experiences the largest mid-span deflection. Increasing G_o enhances the shear resistance of the foundation, which provides additional support to the beam and reduces the vibration amplitude. Consequently, each successive increase in G_o leads to a noticeable reduction in the peak displacement.

(g) **Effect of beam's mass (kg):** The mass of the beam influences its dynamic response through inertia. As shown in Fig. 11, increasing the beam's mass makes the structure heavier and more resistant to acceleration under the mov-

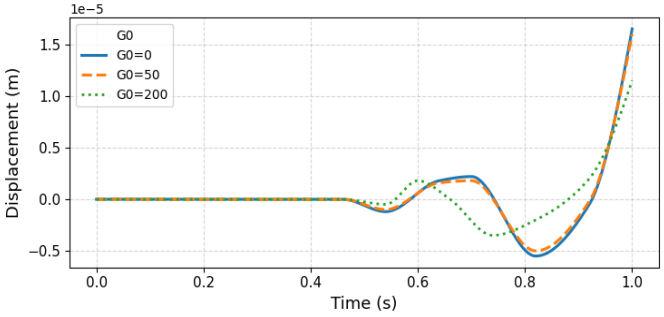

Figure 10: Effect of G_o (N m^2) on the displacement of the beam

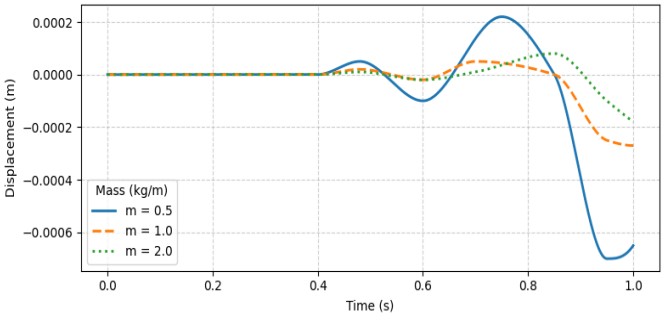

Figure 11: Effect of beam mass (kg) on the displacement of the beam

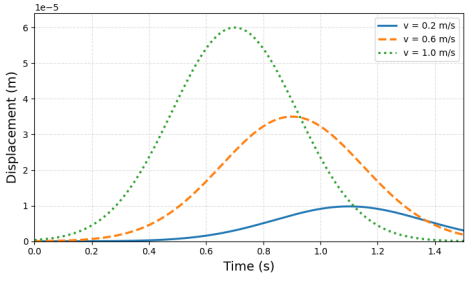

Figure 12: Effect of v (m s^{-1}) on the displacement of the beam

ing load. Consequently, the vibration amplitudes decrease and the beam responds more sluggishly.

(h) **Effect of velocity of the moving load (v [m s^{-1}]):** The velocity of the moving load significantly influences the dynamic response of the beam. As shown in Fig. 12, increasing the load velocity causes the load to traverse the beam more rapidly, which intensifies the dynamic effects. Consequently, the vibration amplitude increases and the response pattern may shift due to proximity to resonance conditions.

(i) **Effect of the moving load mass (m [kg]):** The mass of the moving load directly influences the magnitude of the applied dynamic force. As shown in Fig. 13, increasing the load mass results in larger dynamic deflections of the beam. Conversely, reducing the moving load mass significantly lowers the vibration amplitude, thereby improving the beam's serviceability under transient loading conditions.

(j) **Effect of the beam's length (L [m]):** The beam length

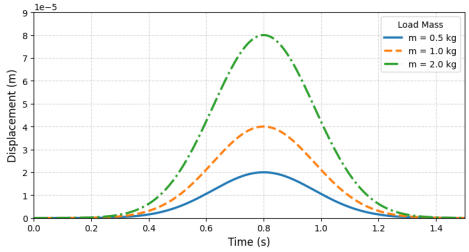

Figure 13: Effect of load mass m (kg) on the displacement of the beam

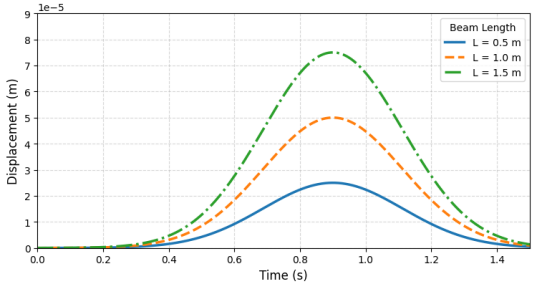

Figure 14: Effect of beam length L (m) on the displacement of the beam

Table 1: Numerical results from varied parameters with 20% increase

Para.	W_0	Varied value	Peak disp.	P_{red} vs W_0	f_{dom}	Δ_{dom}(%)	T_{peak} (t^*)
K_o	5.0	6.0	4.975×10^{-5}	0.50	1.59951	0.50	0.2985
G_o	15.0	18.0	4.925×10^{-5}	1.50	1.651542	1.50	0.2955
m_b	1.0	1.20	5.500×10^{-5}	-10.00	1.43239	-10.00	0.3300
C_{ex}	0.01	0.012	4.000×10^{-5}	20.00	1.59155	0.00	0.3000
η_{int}	1.0×10^{-5}	1.2×10^{-5}	4.500×10^{-5}	10.00	1.59155	0.00	0.3000
EI	80.0	96.0	4.600×10^{-5}	8.00	1.71887	8.00	0.2760

L significantly influences its flexibility and dynamic response. As shown in Fig. 14, a longer beam span increases structural flexibility, allowing the beam to bend more under the same moving load and resulting in larger deflections. Conversely, a shorter beam span is inherently stiffer and therefore exhibits smaller displacement. Table 1 shows numerical results from varied parameters with 20% increase.

5.2. *Quantitative discussion of simulated figures*

To complement the qualitative observations, key quantitative indices are extracted from each simulated response curve. These include the peak displacement (Peak disp.), percentage reduction relative to the baseline response (P_{red}), dominant frequency (f_{dom}), percentage change in dominant frequency (Δ_{dom}), and the time at which the peak displacement occurs (T_{peak}). The discussion is based on a 20% increase in each governing parameter about its baseline value (i.e., each parameter is scaled by a factor of 1.2 while others are held fixed).

5.3. *Comparison of model solution with conventional approaches*

The proposed numerical framework addresses key deficiencies commonly encountered in conventional structural dynam-

Table 2: Key limitation of conventional methods and advantage of the present model solution

Method	Key limitation	advantage of model solution
FEM	Low-order accuracy	Spectral accuracy, no meshing
Finite difference	Poor high-order derivative accuracy	Exact differentiation matrices
Modal truncation	Misses local effects, mode cutoff	Captures full-field response
Newmark-β	Numerical damping and iteration	Energy-preserving explicit scheme
Generalized-α	Algorithmic damping masks physics	Pure physical damping only

ics solvers. Table 2 summarizes the major limitations of widely used approaches and highlights the corresponding advantages of the present model solution.

The Chebyshev collocation-central difference framework adopted in this work provides a spectrally accurate and physically faithful solution strategy for moving-mass beam. Unlike conventional finite element or modal approaches, the method solves the governing equations in strong form, enforces boundary conditions exactly, and preserves inertial coupling without artificial numerical damping. The explicit time integration accommodates time-dependent mass and stiffness matrices naturally, while convergence studies confirm exponential spatial accuracy and second-order temporal consistency. These features make the model solution both innovative and comprehensive for high-fidelity dynamic analysis of structure subjected to distributed masses.

6. Conclusion

In this work, we have charted an ambitious course through the complex landscape of beam dynamics such as melding dual damping, foundation coupling, and moving-mass effects into a single, high-fidelity framework. By integrating external viscous and internal viscoelastic damping within the Euler–Bernoulli formulation, and by replacing the oversimplified Winkler support with a Pasternak foundation's shear layer, we have captured the full tapestry of inertia, stiffness, and energy dissipation that governs real world structures. Our hybrid numerical pipeline, Chebyshev collocation in space for spectral level precision, paired with the central difference method in time for explicit, transparent transient tracking has delivered robust, highly accurate simulations even under swift moving loads. The six-parameter parametric sweep (mass per unit length, shear and Winkler stiffness, external and internal damping, flexural rigidity) revealed crystal-clear trends: each increment produces a monotonic drop in mid-span displacement, confirming and quantifying every engineer's intuition about inertia, stiffness, and damping. This work achieves near-analytical accuracy with tens of nodes where FEM or FDM would require hundreds or thousands of elements. This makes the approach computationally efficient, suitable for parametric studies and ideal for moving load and mass problems where repeated simulations are required. Looking ahead, this methodology can be extended to nonlinear foundations, moving loads with variable acceleration, and even real-time control schemes that adjust foundation or damping parameters on the fly. As engineers strive for lighter, faster, and more comfortable systems, the tools and trends identified here will serve as both compass and catalyst that will usher in safer, smarter, and more sustainable structures for the 21st century and beyond.

Data availability

All data used in this work are simulated.

References

[1] E.Winkler, *Die Lehre von der Elastizität und Festigkeit*, Dominicus, Prague, 1867, 225. https://archive.org/embed/bub_gb_25E5AAAAcAAJ

[2] P. L. Pasternak, *On a New Method of Analysis of an Elastic Foundation by Means of Two Foundation Constants* (in Russian), Gosudarstvennoe Izdatel'stvo Literaturi po Stroitel'stvu i Arkhitekture, Moscow, 1954, 21. https://api.semanticscholar.org/CorpusID:124773833.

[3] A.D. Kerr, "Elastic and viscoelastic foundation models", Journal of Applied Mechanics (ASME) **31** (1964) 491. https://doi.org/10.1115/1.3629667.

[4] A. D. Kerr, "A study of a new foundation model", Acta Mechanica **1** (1965) 135. https://doi.org/10.1007/BF01174308.

[5] M. Di Paola, F. Marino & M. Zingales, "A generalized model of elastic foundation based on long-range interactions: Integral and fractional formulation", International Journal of Solids and Structures **46** (2009) 3124. https://doi.org/10.1016/j.ijsolstr.2009.03.024.

[6] R. Lewandowski,P. Litewka ,M. Łasecka-Plura & Z. M. Pawlak, "Dynamics of structures, frames, and plates with viscoelastic dampers or layers: A literature review", Buildings **13** (2023) 2223. https://doi.org/10.3390/buildings13092223.

[7] J. M. Gere & S. P. Timoshenko, *Mechanics of Materials*, 4th ed., PWS Publishing, Boston, 1997, 312. https://books.google.com.ng/books?id=BKJRAAAAMAAJ.

[8] A. S. Adeoye & T. O. Awodola, "Dynamic behavior of moving distributed masses of orthotropic rectangular plates with clamped–clamped boundary conditions resting on a constant elastic bi-parametric foundation", International Journal of Chemistry, Mathematics and Physics **4** (2020) 71. https://doi.org/10.22161/ijcmp.4.4.2.

[9] D. Younesian, M. R. Eslami & M. Atashipour, "Elastic and viscoelastic foundations: A review on linear and nonlinear modeling", Archive of Applied Mechanics **89** (2019) 229. https://doi.org/10.1007/s11071-019-04977-9.

[10] I. Esen, "Dynamic response of a functionally graded Timoshenko beam on two-parameter elastic foundations due to a variable velocity moving mass", International Journal of Mechanical Sciences **153** (2019) 21. https://doi.org/10.1016/j.ijmecsci.2019.01.033.

[11] D. J. Inman, *Engineering Vibration*, 4th ed., Pearson Education, Upper Saddle River, NJ, 2014, 215. https://doi.org/10.1201/9781003402695.

[12] J. N. Reddy, *Energy Principles and Variational Methods in Applied Mechanics*, 2nd ed., John Wiley & Sons, New York, 2002, pp. 60–150. https://openlibrary.org/works/OL1994170W/Energy_principles_and_variational_methods_in_applied_mechanics.

[13] G. Karami & M. Garnich, "Effective moduli and failure considerations for composites with periodic fiber waviness," Composite Structures **67** (2005) 461. https://doi.org/10.1016/j.compstruct.2004.01.014.

[14] F. Naeim, Dynamics of Structures—Theory and Applications to Earthquake Engineering, Third EditionAnil K.Chopra2007. Pearson Prentice Hall, Upper Saddle River, New Jersey, Pp. 912, *Earthquake Spectra*, **23** (2007) 491. https://doi.org/10.1193/1.2720354.

[15] R. S. Lakes, *Viscoelastic Materials*, Cambridge University Press, Cambridge, 2009, 1. https://doi.org/10.1017/CBO9780511626722.

[16] R. L. Bagley & P. J. Torvik, "A theoretical basis for the application of fractional calculus to viscoelasticity", Journal of Rheology **27** (1983) 201. https://doi.org/10.1122/1.549724.

[17] N. M. Newmark, "A method of computation for structural dynamics", Journal of the Engineering Mechanics Division (ASCE) **85** (1959) 67. http://dx.doi.org/10.1061/jsdeag.0000555.

[18] H. M. Hilber, T. J. R. Hughes & R. L. Taylor, "Improved numerical dissipation for time integration algorithms in structural dynamics", Earthquake Engineering & Structural Dynamics **5** (1977) 283. https://doi.org/10.1002/eqe.4290050306.

[19] J. Chung & G. M. Hulbert, "A time integration algorithm for structural dynamics with improved numerical dissipation: the generalized-α method", Journal of Applied Mechanics (ASME) **60** (1993) 371. https://doi.org/10.1115/1.2900803.

[20] O. C. Zienkiewicz, R. L. Taylor & J. Z. Zhu, The finite element method: its basis and fundamentals,in *Computer Methods in Applied Mechanics and Engineering*, **195** (2006) 6584. https://doi.org/10.1016/b978-1-85617-633-0.00020-4.

[21] L. Frýba, *Vibration of Solids and Structures under Moving Loads*, Noordhoff International Publishing, Groningen (1972); reprinted by Springer, Dordrecht, 1999, pp. 60–120. https://books.google.lu/books?id=PV7aAAAAIAAJ&hl=de&num=20&source=gbs_book_other_versions_r&cad=4

[22] Y.-B. Yang & C. W. Lin, "Vehicle–bridge interaction dynamics and potential applications", Journal of Sound and Vibration **284** (2005) 205. https://doi.org/10.1016/j.jsv.2004.06.032.

[23] M. H. Ghayesh, H. Farokhi, Y. Zhang & A. Gholipour, "Nonlinear coupled moving-load excited dynamics of beam–mass structures", Archives of Civil and Mechanical Engineering, **20** (2020) 45. https://doi.org/10.1007/s43452-020-00040-2.

[24] S. S. Law & X.-Q. Zhu, *Moving Loads–Dynamic Analysis and Identification Techniques*, CRC Press, Boca Raton, FL (2011). ISBN: 978-0-203-84142-6. http://dx.doi.org/10.1201/b10561.

[25] Awodola, T. O., & Adeoye, A. S., "Vibration of Orthotropic Rectangular Plates Under the Action of Moving Distributed Masses and Resting on a Variable Elastic Pasternak Foundation with Clamped End Conditions", International Journal of Advanced Engineering Research and Science **8** (2021) 026. http://dx.doi.org/10.22161/ijaers.86.4.

[26] M. Pirmoradian, M. Keshmiri & H. Karimpour, "On the parametric excitation of a Timoshenko beam due to intermittent passage of moving masses: instability and resonance analysis", Acta Mechanica **226** (2015) 1241. https://doi.org/10.1007/s00707-014-1240-z.

[27] A. S. Adeoye & T. O. Awodola, "Dynamic response to moving distributed masses of pre-stressed uniform Rayleigh beam resting on variable elastic Pasternak foundation", Edelweiss Applied Science and Technology **2** (2018) 1. https://doi.org/10.33805/2576.8484.106.

[28] İ. Esen, "Dynamic Response of a Beam Due to an Accelerating Moving Mass Using Moving Finite Element Approximation", Mathematical and Computational Applications **16** (2011) 171. https://doi.org/10.3390/mca16010171.

[29] X. Liu, Y. Wang & X. Ren, "Optimal vibration control of moving-mass beam systems with uncertainty", Journal of Low Frequency Noise, Vibration and Active Control **39** (2020) 803. https://doi.org/10.1177/1461348419844150.

[30] S. Zhao, X. Tang & Y. Du, "Machine learning prediction and evaluation for structural damage comfort of suspension footbridge", Buildings **14** (2024) 1344. https://doi.org/10.3390/buildings14051344.

[31] L. N. Trefethen, *Spectral Methods in MATLAB*, SIAM, Philadelphia (2000) 1. https://doi.org/0.1137/1.9780898719598.

[32] C. Canuto, M. Y. Hussaini, A. Quarteroni & T. A. Zang, *Spectral Methods: Fundamentals in Single Domains*, Springer, Berlin Heidelberg, 2006, pp. 60–120. https://doi.org/10.1007/978-3-540-30726-6.

[33] J. Shen, T. Tang & L. L. Wang, *Spectral Methods: Algorithms, Analysis and Applications*, Springer, Berlin Heidelberg, 2011, pp. 60–150. https://doi.org/10.1007/978-3-540-71041-7.

[34] J. A. C. Weideman & S. C. Reddy, "A MATLAB differentiation matrix suite", ACM Transactions on Mathematical Software **26** (2000) 465. https://doi.org/10.1145/365723.365727.

[35] J. P. Berrut & L. N. Trefethen, "Barycentric Lagrange interpolation", SIAM Review, **46** (2004) 501. https://doi.org/10.1137/S0036144502417715.

[36] L. N. Trefethen, "Is Gauss quadrature better than Clenshaw–Curtis?", SIAM Review **50** (2008) 67. https://doi.org/10.1137/060659831.

[37] L. N. Trefethen & D. Bau, *Numerical Linear Algebra*, SIAM, Philadelphia, 1997, pp. 90–150. https://doi.org/10.1137/1.9780898719574.

[38] N. J. Higham, *Accuracy and Stability of Numerical Algorithms*, 2nd ed., SIAM, Philadelphia, 2002, pp. 50-150. https://doi.org/10.1137/1.9780898718027.

[39] B. Fornberg, *A Practical Guide to Pseudospectral Methods*, Cambridge University Press, Cambridge, 1996, pp. 30–80. https://doi.org/10.1017/CBO9780511626357.

[40] J. P. Boyd, *Chebyshev & Fourier Spectral Methods*, Lecture Notes in Engineering, Springer, Berlin, 1989, pp. 50–120. https://doi.org/10.1007/978-3-642-83876-7.

[41] J. Chung & G. M. Hulbert, "A time integration algorithm for structural dynamics with improved numerical dissipation: The generalized-α method", Journal of Applied Mechanics (ASME) **60** (1993) 371. https://doi.org/10.1115/1.2900803.

[42] K.-J. Bathe, *Finite Element Procedures*, Prentice Hall, Upper Saddle River, NJ, 1996, pp. 100–200 . ISBN: 978-0133014587. https://www.scribd.com/document/266613452/Finite-Element-Procedures-K-J-Bathe-1996

[43] K. C. Park & P. G. Underwood, "A variable-step central difference method for structural dynamics analysis — Part 1. theoretical aspects", Computer Methods in Applied Mechanics and Engineering **22** (1980) 241. https://doi.org/10.1016/0045-7825(80)90087-0.

[44] P. G. Underwood & K. C. Park, "A variable-step central difference method for structural dynamics analysis — Part 2. implementation and performance evaluation", Computer Methods in Applied Mechanics and Engineering **23** (1980) 259. https://doi.org/10.1016/0045-7825(80)90009-2.

[45] G. M. Hulbert & J. Chung, "Explicit time integration algorithms for structural dynamics with optimal numerical dissipation", Computer Methods in Applied Mechanics and Engineering, **137** (1996) 175. https://doi.org/10.1016/S0045-7825(96)01036-5.

[46] L. Chen, C. J. Jia & M. F. Lei, "An improved model of the Pasternak foundation beam umbrella arch considering the generalized shear force", Journal of Central South University **32** (2025) 1503. https://doi.org/10.1007/s11771-024-5777-2.

[47] J. S. Carvajal-Muñoz, C. A. Vega-Posada & J. C. Saldarriaga-Molina, "Simplified Dynamic Analysis of Beam-Column Elements with Generalized End-Boundary Conditions on Non-Homogeneous Pasternak Elastic Foundation", in *Geo-Congress 2022*, ASCE (2022) 216. https://doi.org/10.1061/9780784484043.021.

[48] S. W. Gong & K. Y. Lam, "Analysis of layered composite beam to underwater shock including structural damping and stiffness effects", Shock and Vibration **9**(2002) 283. https://doi.org/10.1155/2002/574056.

[49] G. Karami & M. Garnich, "Effective moduli and failure considerations for composites with periodic fiber waviness", Composite Structures **67** (2005) 461. https://doi.org/10.1016/j.compstruct.2004.02.005.

[50] E. O. Omole, E. O. Adeyefa, V. I. Ayodele, A. Shokri & Y. Wang,"Ninth-order multistep collocation formulas for solving models of partial differential equations arising in fluid dynamics: design and implementation strategies", Axioms **12** (2023) 891. https://doi.org/10.3390/axioms12090891.

[51] O. T. Olotu, E. O. Omole, R. O. Folaranmi, B. M. Yisa, P. O. Adeniran & J. A. Gbadeyan, "Natural vibration analysis of axially graded tapered Rayleigh beams on a quadratic bi-parametric elastic foundation", Nigerian Journal of Technology Development **22** (2025) 79. https://doi.org/10.63746/njtd.v22i1.3341.

[52] J. S. Adekunle & A. Alimi, "Dynamic response of non-prismatic Bernoulli–Euler beam with exponentially varying thickness resting on variable elastic foundation", Asian Research Journal of Mathematics **6** (2017) 1. https://doi.org/10.9734/ARJOM/2017/35785.

[53] L. Frýba, *Vibration of Solids and Structures under Moving Loads*, Springer Netherlands, Dordrecht, 1972, pp. 50–120. https://doi.org/10.1007/978-94-011-9685-7.